

Let's keep brainstorming title ideas. I don't think our results support the idea of 'episodes of rapid expansion'

Trevor Drees^{*a,b}, Brad M. Ochocki^b, Scott L. Collins^c, and Tom E.X. Miller^b

^aDepartment of Biology, Penn State University, State College, PA USA

^bProgram in Ecology and Evolutionary Biology, Department of BioSciences, Rice University, Houston, TX USA

^cDepartment of Biology, University of New Mexico, Albuquerque, NM USA

April 18, 2021

^{*}thd5066@psu.edu

1 Abstract

2 **Encroachment**¹ of shrubs into adjacent grasslands has become an increasingly reported
3 phenomenon across the world, and such encroachment is either pulled forward by high
4 population growth at the low-density encroachment front or pushed forward by higher-
5 density areas behind the front. However, at sites such as Sevilleta National Wildlife
6 Refuge in central New Mexico, little is known about whether encroachment is pushed or
7 pulled, and the dynamics of encroachment are not well-understood. Here, long-term en-
8 croachment of creosotebush (*Larrea tridentata*), a native perennial shrub, stands in stark
9 contrast with the stagnation in encroachment observed in recent decades. In order to
10 better understand creosotebush encroachment at this site, we quantify it using a spatially
11 structured population model where a wave of individuals travels at a speed governed by
12 both dispersal and density-dependence. Results indicate that population growth rates
13 generally increase with decreasing density, suggesting that encroachment is pulled by
14 individuals at the low-density wave front, and the spatial population model predicts an
15 encroachment rate of less than 2 cm per year. While the predicted rate of encroach-
16 ment is consistent with observations over recent decades, it does not explain long-term
17 creosotebush encroachment at the study site, suggesting that this process may occur in
18 pulses when recruitment, seedling survival, or dispersal significantly exceed typical rates.
19 Overall, our work demonstrates that individuals at low densities are likely the biggest
20 contributors to creosotebush encroachment at this site, and that this encroachment is
21 likely a process that occurs in large but infrequent bursts rather than at a steady pace.

22 Keywords

23 density-dependence, ecotones, woody encroachment, shrubs, integral projection model,
24 grassland

¹*I am not editing the abstract for now.*

25 Introduction

26 The recent and ongoing encroachment of shrubs and other woody plants into adjacent
27 grasslands has caused significant vegetation changes across arid and semi-arid landscapes
28 worldwide (Van Auken, 2000, 2009; Goslee et al., 2003; Gibbens et al., 2005; Parizek et al.,
29 2002; Cabral et al., 2003; Trollope et al., 1989; Roques et al., 2001). The process of en-
30 croachment generally involves increases in the number or density of woody plants in both
31 time and space (Van Auken, 2000), which can drive shifts in plant community structure
32 and alter ecosystem processes (Schlesinger et al., 1990; Ravi et al., 2009; Schlesinger
33 and Pilmanis, 1998; Knapp et al., 2008). Other effects of encroachment include changes
34 in ecosystem services (Reed et al., 2015; Kelleway et al., 2017), declines in biodiversity
35 (Ratajczak et al., 2012; Sirami and Monadjem, 2012; Brandt et al., 2013), and economic
36 losses in areas where the proliferation of shrubs adversely affects grazing land and pastoral
37 production (Mugasi et al., 2000; Oba et al., 2000).

38 Woody plant encroachment can be studied through the lens of spatial population
39 biology as a wave of individuals that may expand across space and over time (Kot et al.,
40 1996; Neubert and Caswell, 2000; Wang et al., 2002; Pan and Lin, 2012). Theory pre-
41 dicts that the speed of wave expansion depends on two processes: local demography and
42 dispersal of propagules. First, local demographic processes include recruitment, survival,
43 growth, and reproduction, which collectively determine the rate at which newly colonized
44 locations increase in density and produce new propagules. Second, colonization events
45 are driven by the spatial dispersal of propagules, which is commonly summarized as a
46 probability distribution of dispersal distance, or “dispersal kernel”. The speed at which
47 expansion waves move is highly dependent upon the shape of the dispersal kernel, espe-
48 cially long-distance dispersal events in the tail of the distribution (Skarpaas and Shea,
49 2007). Both demography and dispersal may depend on plant size, since larger plants
50 often have improved demographic performance and release seeds from greater heights,

51 leading to longer dispersal distances (Nathan et al., 2011). Accounting for population
52 structure, including size structure, may therefore be important for understanding and
53 predicting wave expansion dynamics (Neubert and Caswell, 2000).

54 Theory predicts that the nature of conspecific density dependence is another critical
55 feature of expansion dynamics but this is rarely studied in the context of woody plant
56 encroachment. Expansion waves typically correspond to gradients of conspecific density
57 – high in the back and low at the front – and demographic rates may be sensitive to
58 density due to intraspecific interactions like competition or facilitation. If the demo-
59 graphic effects of density are strictly negative due to competitive effects that increase
60 with density then demographic performance is maximized as density goes to zero, at the
61 leading edge of the wave. Under these conditions, the wave is “pulled” forward by indi-
62 viduals at the low-density vanguard (Kot et al., 1996), and targeting these individuals
63 and locations would be the most effective way to slow down or prevent encroachment
64 (cite?). However, woody encroachment systems often involve positive feedbacks whereby
65 shrub establishment modifies the environment in ways that facilitate further shrub re-
66 cruitment. For example, woody plants can modify their micro-climates in ways that
67 elevate nighttime minimum temperatures, promoting conspecific recruitment and sur-
68 vival for freeze-sensitive species (D’Odorico et al., 2010; Huang et al., 2020). Such Allee
69 effects (in the language of population biology) cause demographic rates to be maximized
70 at higher densities behind the leading edge, which “push” the expansion forward, leading
71 to qualitatively different dynamics (Kot et al., 1996; Taylor and Hastings, 2005; Sullivan
72 et al., 2017; Lewis and Kareiva, 1993; Veit and Lewis, 1996; Keitt et al., 2001). Pushed
73 expansion waves generally have different shapes (steeper density gradients) and slower
74 speeds than pulled waves (Gandhi et al., 2016), and may require different strategies for
75 managing or decelerating expansion (check Taylor and Hastings ref). The potential for
76 positive feedbacks is well documented in woody encroachment systems but it remains
77 unclear whether and how strongly these feedbacks decelerate shrub expansion and influ-

78 ence strategies for management of woody encroachment. Despite decades of work on this
79 topic, we still do not know whether expansion waves of woody encroachment are pushed
80 or pulled.

81 In this study, we linked woody plant encroachment to ecological theory for invasion
82 waves, with the goals of understanding how seed dispersal and density-dependent demog-
83 raphy drive encroachment, and determining whether the encroachment wave is pushed or
84 pulled. Throughout the aridlands of the southwestern United States, shrub encroachment
85 into grasslands is well documented (cite) but little is known about the dispersal and de-
86 mographic processes that govern it. Our work focused on encroachment of creosotebush
87 (*Larrea tridentata*) in the northern Chihuahuan Desert. Expansion of this species into
88 grasslands over the past 150 years has been well documented, leading to decreased cover
89 of *Bouteloua eriopoda*, the dominant foundation species of Chihuahuan desert grassland
90 (Gardner, 1951; Buffington and Herbel, 1965; Gibbens et al., 2005). As in many woody
91 encroachment systems, creosotebush expansion generates ecotones marking a transition
92 from dense shrubland to open grassland, with a transition zone in between where shrubs
93 can often be found interspersed among grasses (Fig. 1).

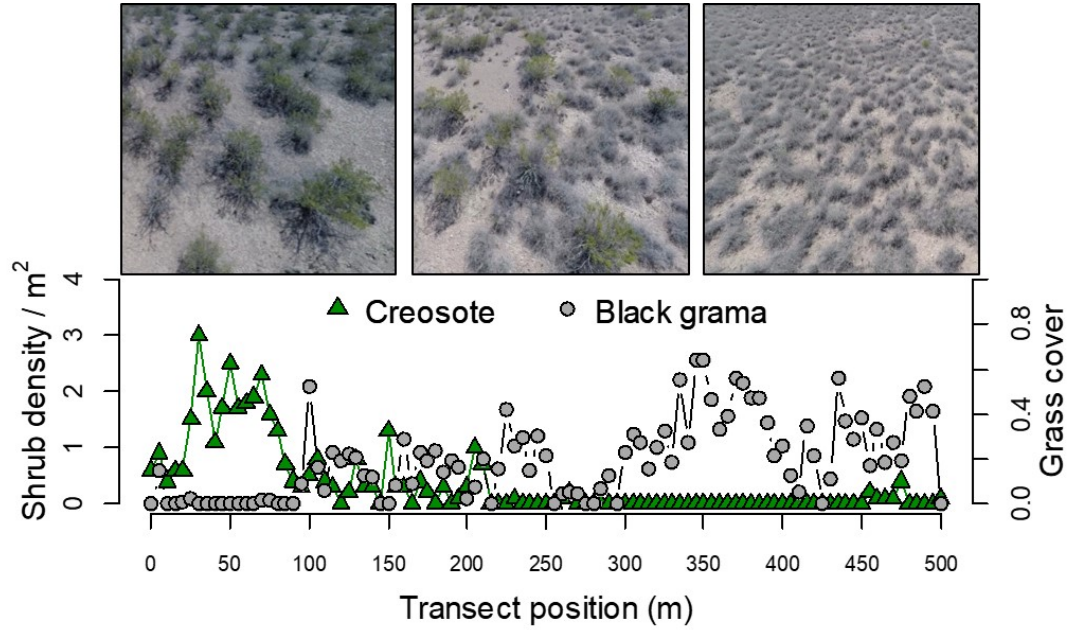


Figure 1: Caption.

94 Historically, creosotebush encroachment into grasslands is believed to have been
 95 driven by a combination of factors including overgrazing, drought, variability in rain-
 96 fall, and suppression of fire regimes Moreno-de las Heras et al. (2016). These shrubs
 97 are also thought to further facilitate their own encroachment through positive feedbacks
 98 (Grover and Musick, 1990; D’Odorico et al., 2012) by modifying their environment in ways
 99 that favor continued growth and recruitment, such as the local micro-climate (D’Odorico
 100 et al., 2010) and rates of soil erosion (Turnbull et al., 2010). Such positive feedback
 101 also involve suppression of herbaceous competitors, reducing competition as well as the
 102 amount of flammable biomass used to fuel the fires that keep creosotebush growth in
 103 check (Van Auken, 2000). We hypothesized that, given potential for positive feedback
 104 mechanisms, the rarity of conspecifics at the low-density encroachment front may depress
 105 demographic performance and generate pushed-wave dynamics.

106 We used a combination of observational and experimental data from shrub ecotones

107 in central New Mexico to parameterize a spatial integral projection model (SIPM) that
 108 predicts that speed of encroachment (m/yr) resulting from lower-level demographic and
 109 dispersal processes. Our data came from demographic surveys and experimental trans-
 110 plants along replicate ecotone transects spanning a gradient of shrub density and seed
 111 drop experiments to infer the properties of the dispersal kernel. We focused on wind
 112 dispersal of seeds as a starting point, since little is known about the natural history
 113 of dispersal in this system and the seeds lack rewards to attract animal dispersers. We
 114 also used re-surveys of permanent transects as an independent measure of encroachment
 115 that provided a benchmark against which to evaluate model predictions. The SIPM ac-
 116 counts for size-structured demography of creosotebush, allows us to test whether shrub
 117 expansion is pulled by the low-density front or pushed from the high-density core, and
 118 identifies the local (demographic) and spatial (seed dispersal) life cycle transitions that
 119 most strongly contribute to expansion speed². We address the following specific ques-
 120 tions:

- 121 1. What is the observed rate of creosotebush encroachment in recent past?
- 122 2. How do creosotebush size and conspecific density affect variation in demographic
 123 vital rates (survival, growth, reproduction, and recruitment) along shrub encroach-
 124 ment ecotones?
- 125 3. What is the wind dispersal kernel for this species and how far do seeds typically
 126 travel by wind?
- 127 4. What is the predicted rate of expansion from the SIPM and what lower-level pro-
 128 cesses most strongly govern the expansion speed?
- 129 5. Is encroachment pulled by the individuals at the front of the wave or pushed by
 130 individuals behind it?

²*we will need to stay consistent with the language of encroachment/expansion/invasion. For now I am swictihg a lot.*

131 **Materials and methods**

132 **Study species**

133 Creosotebush *Larrea tridentata* is a perennial, drought-resistant shrub that is native to
134 the arid and semiarid regions of the southwestern United States and northern Mexico.
135 These shrubs are often found in valleys and on dunes and gentle slopes (Marshall, 1995).
136 High-density areas of creosotebush consist largely of barren soil between plants due to
137 the “islands of fertility” these shrubs create around themselves (Schlesinger et al., 1996;
138 Reynolds et al., 1999), though lower-density areas will often contain grasses in the in-
139 tershrub spaces (Fig. 1). In our northern Chihuahuan desert study region creosotebush
140 reproduces sexually, with numerous small yellow flowers giving rise to highly pubescent
141 spherical fruits several millimetres in diameter; these fruits consist of five carpels, each
142 of which consists of a single seed. Seeds are dispersed from the parent plant by gravity
143 and wind, with the possibility for seeds to also be blown across the soil surface or trans-
144 ported by water runoff (Maddox and Carlquist, 1985). In other regions, this species also
145 reproduces asexually and can give rise to long-lived clonal stands (Vasek, 1980), but this
146 does not occur in our study region. The foliage is dark green, resinous, and unpalatable
147 to most grazing and browsing animals (Mabry et al., 1978).

148 **Study site**

149 We conducted our experiments and censuses at the Sevilleta National Wildlife Refuge
150 (SNWR), a Long-Term Ecological Research (LTER) site in central New Mexico. The
151 refuge exists at the intersection of several eco-regions, including the Chihuahuan Desert
152 and steppes of the Colorado Plateau. Annual precipitation is low at approximately
153 250 mm, with the majority falling during the summer monsoon season from June to
154 September.

155 Significant creosotebush encroachment at SNWR is believed to have last occurred

156 in the 1950's, with high shrub recruitment before and after a multi-year drought that
157 caused a large loss in grass cover, setting the stage for creosotebush expansion (Moreno-
158 de Las Heras et al., 2015; Moreno-de las Heras et al., 2016). The recruitment events
159 that facilitate creosotebush expansion are thought to be highly episodic (Peters and Yao,
160 2012). Given that creosotebush seedlings have been shown to establish around the time
161 that late-summer heavy rainfall occurs (Boyd and Brum, 1983; Bowers et al., 2004),
162 higher precipitation rates may be responsible for increased recruitment.

163 **Encroachment re-surveys**

164 We recorded shrub percent cover along two permanent 1000-m transects that spanned
165 the shrub-grass ecotone, from high to low to near-zero shrub density. These surveys were
166 conducted in summer 2001 and again in summer 2013 to document change in creosotebush
167 abundance and spatial extent. At every 10 meters, shrub cover was recorded in nine cover
168 classes (<1%, 1–4%, 5–10%, 10–25%, 25–33%, 33–50%, 50–75%, 75–95%, >95%). For
169 visualization, we show midpoint values of these cover classes at each meter location for
170 both transects and years.

171 **Demographic data**

172 **Ecotone transects**

173 Collection of demographic data occurred during early June of every year from 2013-2017.
174 This work was conducted at four sites in the eastern part of SNWR (one site was initiated
175 in 2013 and the other three in 2014), with three transects at each site (different transects
176 than those used for re-surveys). All transects were placed along a shrubland-grassland
177 ecotone so that a full range of shrub densities was captured: each transect spanned
178 core shrub areas, grassland with few shrubs, and the transition between them. Lengths
179 of these transects varied from 200 to 600 m, determined by the strength of vegetation
180 transition since “steep” transitions required less length to capture the full range of shrub

181 densities.

182 We quantified shrub density in 5-meter “windows” along each transect, including all
183 plants within one meter of the transect on either side. Densities were quantified once for
184 each transect (in 2013 or 2014) and were assumed to remain effectively constant for the
185 duration of the study, a reasonable assumption for a species with very low recruitment
186 and very high survival of established plants. Given the population’s size structure, we
187 weighted the density of each window by the sizes of the plants, which we quantified as
188 volume (cm³). Volume was calculated as that of an **elliptic**³ cone: $V_i = \pi lwh/3$ where l ,
189 w , and h are the maximum length, maximum width, and height, respectively. Maximum
190 length and width were measured so that they were always perpendicular to each other,
191 and height was measured from the base of the woody stem at the soil surface to the
192 highest part of the shrub. The weighted density for a window was then expressed as
193 $\log(\text{volume})$ summed over all plants in the window.

194 **Observational census**

195 At 50-m intervals along each transect we tagged up to 10 plants for annual demographic
196 census and recorded their local (5-m resolution) window so that we could connect indi-
197 vidual demographic performance to local weighted density. These tagged shrubs were
198 revisited every June and censused for survival (alive/dead), size (width, length, and
199 height, as above), and reproduction (numbers of flowers and fruits). In instances where
200 shrubs had large numbers of reproductive structures that would be difficult to reliably
201 count (a large shrub may have many hundreds of flowers or fruits), we made counts on a
202 fraction of the shrub and extrapolated to estimate whole-plant reproduction. Creosote-
203 bush does not have a discrete reproductive season, instead producing flowers and fruits
204 over much of the warm season. Our measurements of reproductive output are therefore
205 conservative, and likely underestimate cumulative seed production for an entire transi-

³*I checked the code and actually this is not what we did.*

tion year. Each year, we also searched for new recruits within one m on either side of the transect. New recruits were tagged and added to the demographic census.

Transplant experiment

We conducted a transplant experiment in 2015 to test how shrub density affects seedling survival. This approach complemented observational estimates of density dependence and filled in gaps for a part of the shrub life cycle that is rarely observed due to low recruitment. Seeds for the experiment were collected from plants in our study population in 2014. Seeds were germinated on Pro-Mix potting soil (Quakertown, PA) in Fall 2014 and seedlings were transferred to 3.8 cm-by-12.7 cm cylindrical containers and maintained in a greenhouse at Rice University. Seedlings were transported to SNWR and transplanted into our experimental design during July 27-31 2015. Transplant timing was intended to coincide with the start of the monsoon season, when most natural recruitment occurs.

The transplant experiment was conducted at the same four sites and three transects per site as the observational demographic census, where we knew weight shrub densities at 5-m window resolution. Along each transect we established 12 1-m by 1-m plots. Plots were intentionally placed to capture density variation: four plots were in windows with zero shrubs, four plots were placed in the top four highest-density windows, and the remaining four plots were randomly distributed among the remaining windows with weighted density greater than zero. Plots were placed in the middle of each 5-m window (at meter 2.5). Plots were divided into four 0.5-m by 0.5-m subplots. We divided each subplot into nine squares and recorded ground cover of each square as one of the following categories: bare, creosotebush, black grama (*B. eriopoda*), blue grama (*B. gracilis*), other grass, or “other”. Each subplot received one transplanted subplot, for a total of 48 transplants per transect, 144 transplants per site, and 576 transplants in the entire experiment. Each site was set up on a different day and there was a significant monsoon event after the third and before the fourth site. This resulted in differential mortality

that appears to be related to site (the soil was moist at the fourth site at the time of transplanting, which favored survival) but more likely reflects the timing of the monsoon event relative to planting. We revisited the transplant experiment on October 24, 2015 to survey mortality. After that first visit, transplants were censused along with the naturally occurring plants each June, following the methods described above.

Demographic data analysis

We fit statistical models to the demographic data and used AIC-based model selection to evaluate empirical support for alternative candidate models. The top statistical models were then used as the vital rate sub-models of the SIPM, so there is a strong connection between the statistical and population modeling, as is typical of integral projection modeling. Our analyses focused on the following demographic vital rates: survival, growth, probability of flowering, flower and fruit production, and seedling recruitment. All of these except recruitment were modeled as a function of plant size, and all of them included the possibility of density dependence, since we could connect the demographic performance of individual shrubs to the weighted density of their transect window.

The alternative hypotheses of pushed versus pulled wave expansion ultimately rest on how demographic vital rates, and the rate of population increase (λ) derived from the combination of all vital rates, respond to density. We were particularly interested in whether demographic performance was maximized as local density goes to zero (pulled) or at non-zero densities behind the wave front (pushed). To flexibly model density dependence and detect non-monotonic responses, we used generalized additive models in the R package ‘mgcv’ (Wood, 2017). For each vital rate, we fit candidate models with or without a smooth term for local weighted density (among other possible covariates). To avoid over-fitting, we set the ‘gamma’ argument of `gam()` to 1.4, which increases the complexity penalty, results in smoother fits (Wood, 2017), and therefore makes our approach more conservative. All models included the random effect of transect; we did

not attempt to model both site and transect-within-site random effects due to the low numbers of each.

Collected demography data were then examined to investigate how weighted density and shrub volume affected four different demographic variables: survival, probability of flowering (i.e. producing at least one flower or fruit), annual growth, and number of reproductive structures. Each of these demographic variables was fit to a different mixed-effects model through maximum likelihood. Both survival and probability of flowering were each fit to generalised linear mixed-effects models using a binomial response and a logit link function. Annual growth was defined as $\ln(V_{t+1}/V_t)$ where V_{t+1} and V_t are the shrub volumes in the current and previous years, respectively, and was then fit to a linear mixed-effects model. The number of reproductive structures was defined as the natural logarithm of the sum of fruits and flowers on the entire shrub and was fit to a linear mixed-effects model as well. To construct these models, all of the equations listed in Table 1 were first fit to each of the four demographic variables, with each equation using volume and standardised density as predictors while also treating the unique transect in which each shrub was located as a random effect. After these equations were fit to the data, all eight equations for each demographic variable were ranked based on their value of the Akaike information criterion (AIC) and weighted based on their quality so that better-fitting models had a higher weight. Then, coefficients of the same type were averaged between all eight models for each demographic variable using a weighted mean corresponding to model quality in order to generate an average model. All four average models have the general form

$$R = \beta_1 v + \beta_2 d + \beta_3 d^2 + \beta_4 vd + \beta_5 vd^2 + \epsilon \quad (1)$$

where R is the response variable, v and d are the volume and density, ϵ is a random transect effect, and β is the coefficient for each type of term.

283 The effect of density dependence on the probability of recruitment from seeds was
 284 also modelled. For every year, the sum of seeds produced the prior year was calculated
 285 for each 5-m subsection, and then probability of recruitment was calculated as the num-
 286 ber of recruits observed in each 5-m subsection divided by that number of seeds. For
 287 any subsection in which seeds were not found, a count of seeds was estimated based on
 288 the number of seeds in a subsection of similar weighted density; this was done to avoid
 289 creating any undefined values of recruitment probability. Both linear and quadratic mod-
 290 els using only weighted density as a predictor were fit to the distribution of recruitment
 291 probabilities, though the linear model was ultimately used because it had a higher AIC
 292 value.

293 **Dispersal modelling**

294 Dispersal kernels were calculated using the WALD, or Wald analytical long-distance
 295 dispersal, model that uses a mechanistic approach to predict dispersal patterns of plant
 296 propagules by wind. The WALD model, which is largely based in fluid dynamics, can
 297 serve as a good approximation of empirically-determined dispersal kernels (Katul et al.,
 298 2005; Skarpaas and Shea, 2007) and may be used when empirical dispersal data is not
 299 readily available. Under the assumptions that wind turbulence is low, wind flow is
 300 vertically homogenous, and terminal velocity is achieved immediately upon seed release,
 301 the WALD model simplifies a Lagrangian stochastic model to create a dispersal kernel
 302 that estimates the likelihood a propagule will travel a given distance (Katul et al., 2005).
 303 This dispersal kernel takes the form of the inverse Gaussian distribution

$$304 \quad p(r) = \left(\frac{\lambda'}{2\pi r^3} \right)^{\frac{1}{2}} \exp \left[-\frac{\lambda'(r - \mu')^2}{2\mu'^2 r} \right] \quad (2)$$

305 that is a slight adaptation from equation 5b in Katul et al. (2005), using r to denote
 306 dispersal distance. Here, λ' is the location parameter and μ' is the scale parameter,

which depend on environmental and plant-specific properties of the study system. The location and scale parameters are defined as $\lambda' = (H/\sigma)^2$ and $\mu' = HU/F$; these are functions of the height H of seed release, wind speed U at seed release height, seed terminal velocity F , and the turbulent flow parameter σ that depends on both wind speed and local vegetation roughness.

In order to create the dispersal kernel, we first take the wind speeds at measurement height z_m and correct them to find wind speed U for any height H by using the logarithmic wind profile

$$U = \frac{1}{H} \int_{d+z_0}^H \frac{u^*}{K} \log \left(\frac{z-d}{z_0} \right) dz \quad (3)$$

given in Bullock et al. (2012) equation 6, with the notation slightly modified. Here, z is the height above the ground, K is the von Karman constant, and u^* is the friction velocity. The zero-plane displacement d and roughness length z_0 are surface roughness parameters that, for a grass canopy height h above the ground, are approximated by $d \approx 0.7h$ and $z_0 \approx 0.1h$. These estimates are from Raupach (1994) for a canopy area index $\Lambda = 1$ in which the sum of grass canopy elements is equal to the unit area being measured. A 0.15 m grass height at the study site gives $d = 0.105$ and z_0 , which are suitable approximations for grassland (Wiernga, 1993). Calculations of u^* were done using equation A2 from Skarpaas and Shea (2007), in which

$$u^* = KU_m \left[\log \left(\frac{z_m - d}{z_0} \right) \right]^{-1} \quad (4)$$

and U_m is the mean wind velocity at the measurement height z_m . Values for the turbulent flow parameter σ were then calculated using the estimate made by Skarpaas and Shea

328 (2007) in their equation A4, where

$$329 \quad \sigma = 2A_w^2 \sqrt{\frac{K(z-d)u^*}{C_0 U}} \quad (5)$$

330 and C_0 is the Kolmogorov constant. A_w is a constant that relates vertical turbulence
 331 to friction velocity and is approximately equal to 1.3 under the assumptions of above-
 332 canopy flow made by Skarpaas and Shea (2007), based off calculations from Hsieh and
 333 Katul (1997). In addition, the assumption that $z = H$ was made in order to make the
 334 calculation of σ more feasible.

335 The values from the previous three equations give us the necessary information to
 336 calculate μ' and λ' , thus allowing us to create the WALD distribution $p(r)$. However, the
 337 base WALD model does not take into account variation in wind speeds or seed terminal
 338 velocities, which limits its applicability in systems where such variation is present. In
 339 order to account for this variation, we integrate the WALD model over distributions these
 340 two variables using the same method as Skarpaas and Shea (2007). The WALD model
 341 assumes seed release from a single point source, though, which is not realistic for a shrub;
 342 because seeds are released across the entire height of the shrub rather than from a point
 343 source, $p(r)$ was also integrated across the uniform distribution from the grass canopy
 344 height to the shrub height. Thus, under the assumptions that the height at which a
 345 seed is located does not affect its probability of being released and that seeds are evenly
 346 distributed throughout the shrub, this gives the dispersal kernel $K(r)$, where

$$347 \quad K(r) = \iiint p(F)p(U)p(z)p(r) dF dU dz \quad (6)$$

348 and $p(F)$ and $p(U)$ are the PDFs of the terminal velocity F and wind speed U , respec-
 349 tively, and $p(z)$ is the uniform distribution from h to H .

350 The distribution $p(F)$ in the integral above was constructed using experimentally
 351 determined seed terminal velocities. This was done by using a high-speed camera and

352 motion tracking software to determine position as a function of time, and then using the
 353 Levenberg-Marquardt algorithm to solve a quadratic-drag equation of motion for F . Be-
 354 fore seeds were released, they were dried and then dyed with yellow fluorescent powder,
 355 and then put against a black background to improve visibility and make tracking easier.
 356 While the powder added mass to the seeds, this added mass only yielded an approxi-
 357 mately 2.5% increase and was thus negligible, likely having little effect on their terminal
 358 velocities. Measurements were conducted for 48 seeds that were randomly chosen from a
 359 seed pool derived from different plants, and then an empirical PDF of terminal velocities
 360 was constructed using the data. Constructing $p(U)$ involved creating an empirical PDF
 361 of hourly wind speeds at Five Points, the site closest to the 12 transects being used,
 362 that were obtained from meteorological data collected at the Sevilleta National Wildlife
 363 Refuge from 1988 to 2010. We did not weight $p(U)$ and assumed that the probability
 364 seed release from the shrub is the same regardless of wind speed.

365 **Spatial integral projection model**

366 Given that the shrub population at this site is approximately homogeneous perpendic-
 367 ular to the direction of encroachment, expansion is modelled as a wave moving in one
 368 dimension. A spatial integral projection model (SIPM) is used to estimate the speed at
 369 which encroachment occurs; such a model incorporates the effects of variation in traits
 370 like plant size that stage-structured models, such as those described in Neubert and
 371 Caswell (2000), do not capture. According to Jongejans et al. (2011), a general SIPM
 372 can be formulated as

$$373 \quad \mathbf{n}(x_2, z_2, t + 1) = \iint \tilde{K}(x_2, x_1, z_2, z_1) \mathbf{n}(x_1, z_1, t) dx_1 dz_1 \quad (7)$$

374 where x_1 and x_2 are locations of individuals of a particular size before and after one unit of
 375 time, and z_1 and z_2 are the respective sizes. The vector \mathbf{n} indicates the population density

of each size, and \tilde{K} is a kernel that combines dispersal with demography. Though this SIPM represents a continuous spectrum of shrub sizes and densities, it was implemented by discretising the above integral with a 200 x 200 matrix, as this makes calculations significantly more tractable.

Movement of the wave is determined by the components of the combined dispersal/demography kernel \tilde{K} , which is of the same form as that used in Jongejans et al. (2011). Here,

$$\tilde{K}(x_2, x_1, z_2, z_1) = K(x_2 - x_1)Q(z_2 - z_1) + \delta(x_2 - x_1)G(z_2 - z_1) \quad (8)$$

and K is the dispersal kernel, Q a reproduction function, G a growth function, and δ the Dirac delta function. G is derived from the model for annual growth ratio, and Q is derived from the reproductive structures model as well as other factors including number of seeds per reproductive structure, probability of recruitment from seed, and recruit size. Both G and Q give the probability of transition between sizes; in the case of G , this is the probability of growing from one specific size to another, and in the case of Q the probability that an individual of a specific size produces a recruit of a specific size. The product of K and Q represents the production and dispersal of motile propagules, while the product of G and δ represents the growth of sessile individuals.

Given growth function G and the reproduction function Q , the speed of the moving wave can be calculated as

$$c^* = \min_{s>0} \left[\frac{1}{s} \ln(\rho_s) \right] \quad (9)$$

where s is the wave shape parameter and ρ_s is the dominant eigenvalue of the kernel \mathbf{H}_s (Jongejans et al., 2011). This estimate for the wavespeed is valid under the assumption that population growth decreases monotonically as conspecific density increases, with the highest rates of growth occurring at the lowest population densities (Lewis et al., 2006).

400 The kernel \mathbf{H}_s is defined as

$$401 \quad \mathbf{H}_s = M(s)Q(z_2 - z_1) + G(z_2 - z_1) \quad (10)$$

402 where $M(s)$ is the moment-generating function of the dispersal kernel (Jongejans et al.,
403 2011). For one-dimensional dispersal, this moment-generating function can be estimated
404 as

$$405 \quad M(s) = \frac{1}{N} \sum_{i=1}^n I_0(sr_i) \quad (11)$$

406 where r is the dispersal distance for each observation, and I_0 is the modified Bessel
407 function of the first kind and zeroth order (Skarpaas and Shea, 2007). In order to obtain
408 M , numerous dispersal distances were simulated from the dispersal kernel $K(r)$ described
409 in the previous section, with over 2000 replications for each shrub height increment of 1
410 cm. This was performed over the range from the lowest possible dispersal height to the
411 maximum shrub height. Once $M(s)$ was obtained for dispersal at each shrub height, \mathbf{H}_s
412 and c^* were calculated for each value of s ; this was done for values of s ranging from 0
413 to 2, as it is this range in which c^* occurs.

414 Estimates of the wavespeed were bootstrapped for a total of 1000 replicates. Each
415 bootstrap replicate recreated size- and density-dependent demographic models using 80%
416 resampling on the original demographic data, and recreated dispersal kernels also using
417 80% resampling on the wind speeds and seed terminal velocities. Between replicates,
418 the structure of the demographic models was kept constant, though coefficient estimates
419 were not; this approach, while effectively ignoring model uncertainty, has the benefit of
420 increasing computational efficiency, which is especially useful given the time-consuming
421 nature of numerically estimating the many dispersal kernels used in the model.

Results

Encroachment re-surveys

Figure 2.

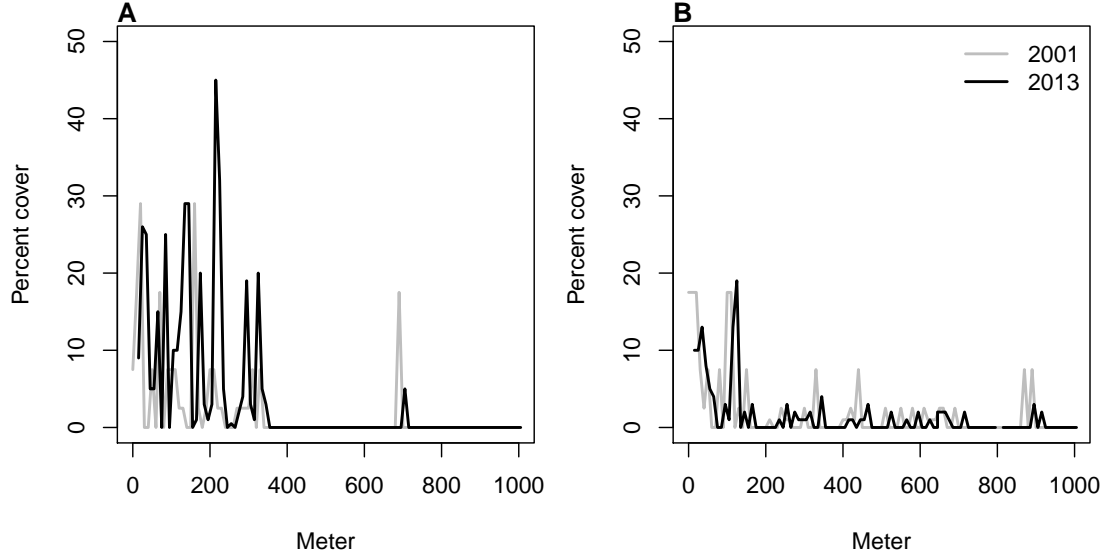


Figure 2: Re-surveys of shrub cover along two permanent transects (A,B) surveyed in 2001 and 2013.

The speed of encroachment at the study site as estimated by the SIPM is rather slow; as can be seen in Figure 3, the low-density wavefront moves at approximately 0.5 cm/yr under normal conditions and at 1 cm/yr under the best seedling survival conditions observed in the dataset. These improved conditions were observed due to above-average rainfall that occurred after greenhouse-grown seedlings were transplanted to the site. Population growth in this low-density region of the moving wave is also low, with a geometric growth rate of $\lambda \approx 1.006$ and even lower rates of growth the higher-density regions behind; in the higher-survival scenario the maximum rate increases to $\lambda \approx 1.013$, with growth still decreasing as density increases. For both scenarios, the decrease in population growth rate with increasing density was monotonic across the range of observed standardised densities, as is shown in Figure 3. This suggests that

436 an Allee effect is likely not present in this population, as the highest rate of population
 437 growth is found at the lowest density vanguard of the encroaching population. Thus, the
 438 conditions necessary for equation 9 to be valid are satisfied, and these wavespeeds are
 439 applicable for a pulled-wave scenario in which no Allee effects are present.

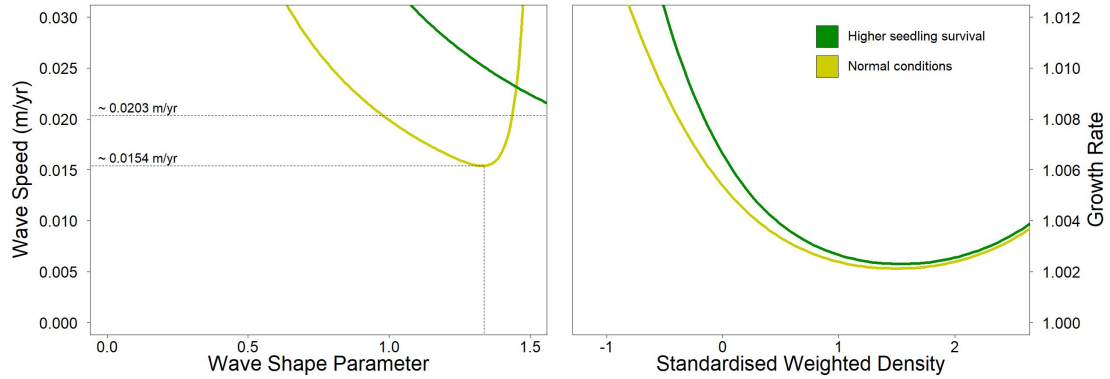


Figure 3: Estimated encroachment wave speeds (left) and geometric rates of population growth (right) for higher post-rainfall seedling survival and normal conditions.

440 As the speed of encroachment is quite limited, so is the extent of wind dispersal.
 441 Long distance dispersal events, while more common for taller shrubs than their shorter
 442 counterparts, are still uncommon overall. For the tallest shrub height of 1.98 m, only
 443 0.32% of propagules exceed a dispersal distance of 5 m, and 0.02% exceed 10 m. At 1
 444 m, or approximately half the tallest shrub height, long distance dispersal is even less
 445 likely, with 0.0046% of propagules exceeding a dispersal distance of 5 m and 0.0009%
 446 exceeding 10 m. Given that the median shrub height is only 0.64 m, the occurrence of
 447 long-distance wind dispersal in most of the shrub population is highly improbable, and
 448 the few instances in which it occurs will only be limited to the tallest shrubs. Thus, as
 449 Figure 4 demonstrates, shorter dispersal distances dominate; even for the tallest shrub,
 450 81% of seeds fall within only a metre of the plant, and this percentage increases as
 451 shrub height decreases. Dispersal kernels have their highest probability density at dis-
 452 persal distances between 2 and 8 cm from the shrub; here, as shrub height increases, the

453 most probable dispersal distance slightly increases while maximum probability density
 454 decreases. Regardless of the shrub height, most dispersal will occur very close to the
 455 plant, though increases in shrub height dramatically increase the likelihood of dispersal
 456 at longer distances. It is clear that the shape of the height-dependent dispersal kernel
 457 $K(r)$ varies greatly among the shrub population given the large range of shrub heights
 458 observed; shrubs at lower heights have more slender kernels with most of the seeds dis-
 459 persing closer to the plant, while taller shrubs have kernels with much fatter tails and
 460 are more capable of longer-distance dispersal.

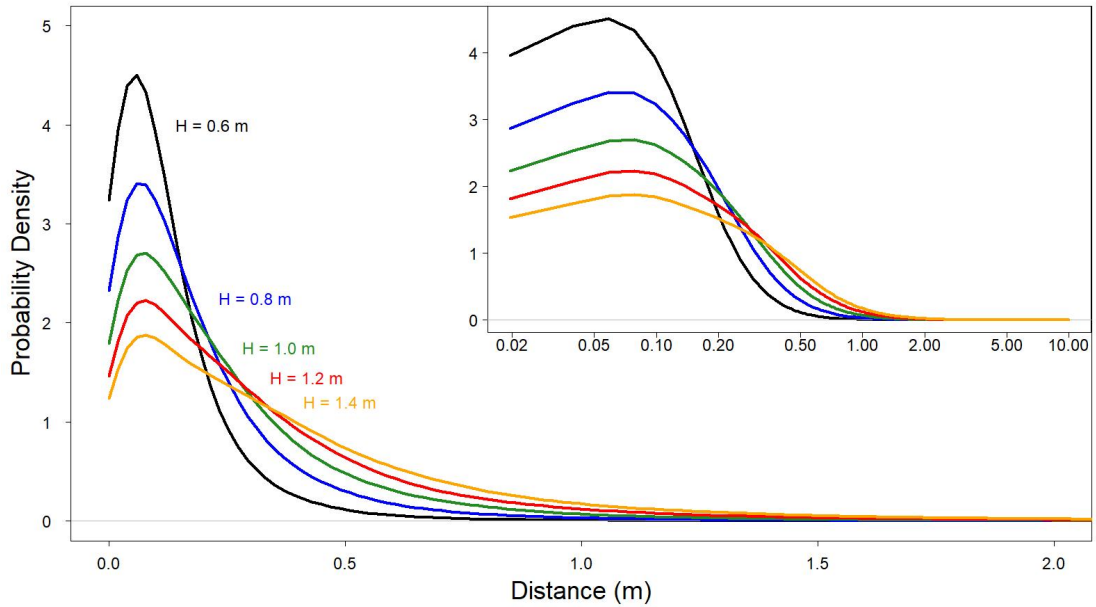


Figure 4: Dispersal kernels, with each colour representing a selected shrub height. The inset plot is the same as the large plot, though with a logarithmic x-axis to more easily show differences in dispersal probability at smaller distances.

461 Density and size dependence are evident in all 4 of the demographic rates, with
 462 coefficients for each model displayed in Table 2. For growth, reproduction, and survival,
 463 density dependence is mostly negative and monotonic; this is not the case for probability
 464 of flowering, where shrub size seems to be more important than the effects of density alone

465 and suggests that larger shrubs have a higher probability of flowering than their smaller
466 counterparts. This, along with size and density dependence in growth and reproduction,
467 is shown in Figure 5. Size dependence is positive for reproduction, as would be expected
468 since larger plants typically produce more flowers and fruits. However, annual growth
469 decreases as size increases; this could be in part due to the annual growth in this study
470 being quantified as a proportion relative to the shrub's initial size. While larger shrubs
471 may produce more plant material over a year in terms of absolute volume, smaller shrubs
472 produce less but can still have higher annual growth in terms of the percentage of volume
473 added relative to their initial volume. When compared to density, shrub size is a much
474 stronger predictor of survival, with significant differences in mortality rates depending on
475 shrub size. For small shrubs, mortality is exceptionally high, and increases in volume for
476 these shrubs only slightly increase the likelihood of survival. However, after shrubs reach
477 a logarithmic volume of approximately 7.3, they are almost guaranteed to survive, with
478 survival rates near 100% persisting regardless of any further size increases. Interestingly,
479 though most recruits were found at lower densities, the probability of recruitment from
480 seed displays positive density dependence; the probability of recruitment was still very
481 low, though, with a baseline rate of approximately 2 recruits per 10,000 seeds.

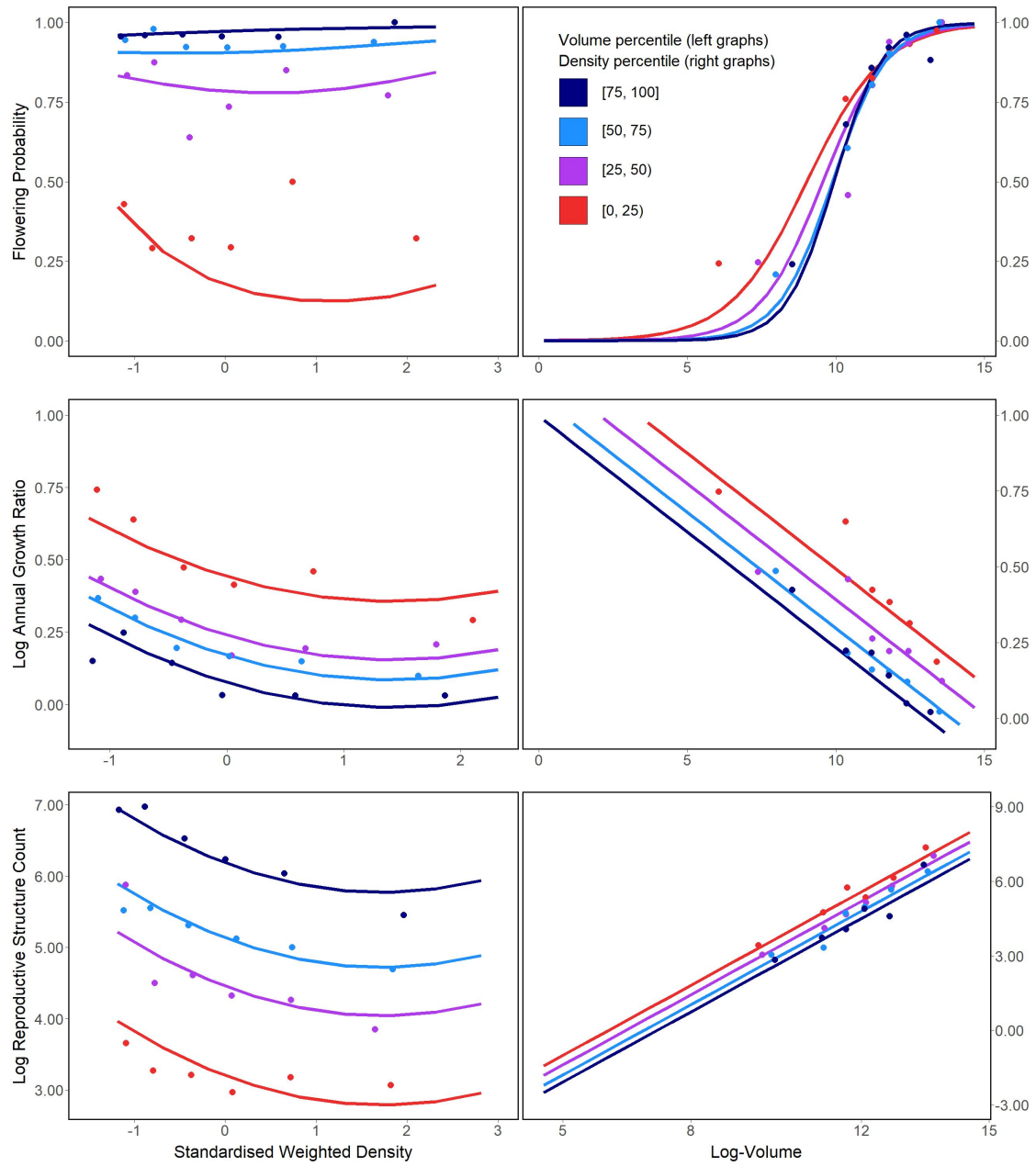


Figure 5: Flowering probability (top row), log annual growth ratio (centre row), and log reproductive structure count (bottom row) at all four sampling sites. In the left column of graphs, the three response variables are shown as a function of density for each of four volume quartiles, with each quartile containing six density bins; in the right column, the opposite occurs, with response variables shown as functions of four volume quartiles that each contain six density bins. Graphs quantifying the number of reproductive structures include data only on plants that flowered.

Discussion

The slow movement of the encroaching creosotebush wave at the Sevilleta LTER site can likely be contributed to a combination of three factors: short dispersal distances with extremely limited long-distance dispersal events, very low probability of recruitment from seed, and high seedling mortality. These three barriers, when combined, form a formidable challenge to the establishment of new shrubs at the low-density front of the wave. First, a seed must travel far enough to avoid competition with the parent shrub, which is unlikely given the dispersal kernels shown in Figure 2. Even if the seed manages to be dispersed this far, its chances of becoming a seedling are low. Caching and consumption by seed-eaters such as a variety of seed-harvesting ants (Whitford, 1978; Whitford et al., 1980; Lei, 1999) and the kangaroo rat *Dipodomys merriami* (Chew and Chew, 1970) decreases the amount of seeds available for germination. However, reduction in germination caused by destruction of seeds may be partly mitigated by the more favourable germination conditions that these seeds can experience when cached underground (Chew and Chew, 1970). Many of the remaining seeds will still fail to germinate, and in the unlikely event that germination does occur, seedlings will likely die given the high rates of mortality observed in smaller shrubs. Such high rates of creosotebush seedling mortality have been observed in other studies as well (Boyd and Brum, 1983; Bowers et al., 2004), probably due to a combination of herbivory, competition, and abiotic stresses.

However, as low as they are, the wavespeed estimates given in this paper are still conservative estimates for reasons mostly related to dispersal. First, it is important to note that the dispersal kernels used here, while they account for variation in factors such as wind speed and terminal velocity, may underestimate the distances that shrub propagules travel. Because the WALD model assumes that terminal velocity is reached immediately upon seed release, seeds in the estimate thus take a shorter time to fall

508 and have less time to be transported by wind, and the true frequency of long-distance
509 dispersal events may thus be greater than what is estimated here. Second, dispersal at the
510 study site could occur through additional mechanisms other than wind. For example,
511 secondary dispersal through runoff from significant rainfall events can transport seeds
512 (Thompson et al., 2014), and given that long-distance dispersal by bird and subsequent
513 species divergence is thought to be responsible for creosotebush being in North America
514 in the first place (Wells and Hunziker, 1976), short-distance dispersal by other animals
515 at the study site likely occurs. As mentioned above, seeds are transported by seed-
516 harvesting ants and granivorous mammals, where they are often stored in caches that
517 can be appreciable distances from the parent shrubs. Whether transportation occurs via
518 ant or rodent, creosotebush seeds can be moved significantly further than wind alone
519 can, though many of these seeds are eventually consumed.

520 Despite the more conservative estimates our model yields, the estimated rate of dis-
521 persal in creosotebush populations at the Sevilleta National Wildlife Refuge is consistent
522 with observations from the past 50-60 years, as creosotebush expansion during this time
523 has been minimal (Moreno-de las Heras et al., 2016). However, it cannot explain the
524 long-term increases in creosotebush cover at the study site, as total encroachment over
525 the past 150 years is much greater than what would be expected given the encroachment
526 rates derived by our models. Such a discrepancy is likely due to much of the expansion
527 occurring in an episodic fashion, with short times during which rapid encroachment oc-
528 curs due to favourable environmental conditions. This could be due in part to seedling
529 recruitment, which is a factor that strongly limits creosotebush expansion, being rare
530 and episodic. For example, Allen et al. (2008) estimate that a major recruitment event
531 occurred at this site in the 1950s, which is supported by photographic evidence from
532 Milne et al. (2003) of a drought-driven expansion during this time. Moreno-de las Heras
533 et al. (2016) estimate that after this expansion, several smaller creosotebush recruitment
534 events occurred in decadal episodes. However, such events can be highly localised and

535 may not necessarily occur at the low-density front of encroachment, which could explain
536 how these recruitment events can still coexist with lack of encroachment in the recent
537 past.

538 Overall, our observations and model highlight three aspects of creosotebush encroach-
539 ment that should be the focus of future studies seeking to obtain better estimates of
540 encroachment rates. First, negative density dependence in survival, growth, and repro-
541 duction is demonstrated, along with size dependence. The clear dependence on size and
542 conspecific density suggests that they both should be considered when estimating cre-
543 osotebush expansion and quantifying the demographic variation that contributes to it.
544 Second, wind dispersal in these shrubs is quite limited; though the dispersal kernels seen
545 here are typical in the sense that they are characterised by high near-plant dispersal and
546 exceptionally low long-distance dispersal, the scale across which such dispersal occurs
547 is small, with most seeds landing within only 1 m of the shrub. Wind dispersal alone
548 may be an underestimate of the true amount of dispersal occurring, and future work
549 should seek to incorporate the effects of dispersal by runoff and animals so that a more
550 representative model of total dispersal can be obtained. Finally, encroachment is slow or
551 even stagnates, but only most of the time. Though our encroachment speed estimates
552 are representative of creosotebush populations for most years, the significant expansion
553 seen over larger time scales suggests that there is episodic expansion in other years; while
554 our model is consistent with the recent stagnation in creosotebush encroachment at the
555 Sevilleta LTER site, a model that also includes interannual variability in factors such
556 as survival and recruitment would be able to better account for instances of episodic
557 population expansion that are characteristic of this location.

558 Acknowledgements

559 Author contributions

560 Data accessibility

561 References

- 562 Allen, A., W. Pockman, C. Restrepo, and B. Milne. 2008. Allometry, growth and
563 population regulation of the desert shrub *Larrea tridentata*. *Functional Ecology* pages
564 197–204.
- 565 Bowers, J. E., R. M. Turner, and T. L. Burgess. 2004. Temporal and spatial patterns in
566 emergence and early survival of perennial plants in the Sonoran Desert. *Plant Ecology*
567 **172**:107–119.
- 568 Boyd, R. S., and G. D. Brum. 1983. Postdispersal reproductive biology of a Mojave Desert
569 population of *Larrea tridentata* (Zygophyllaceae). *American Midland Naturalist* pages
570 25–36.
- 571 Brandt, J. S., M. A. Haynes, T. Kuemmerle, D. M. Waller, and V. C. Radeloff. 2013.
572 Regime shift on the roof of the world: Alpine meadows converting to shrublands in
573 the southern Himalayas. *Biological Conservation* **158**:116–127.
- 574 Buffington, L. C., and C. H. Herbel. 1965. Vegetational changes on a semidesert grassland
575 range from 1858 to 1963. *Ecological monographs* **35**:139–164.
- 576 Bullock, J. M., S. M. White, C. Prudhomme, C. Tansey, R. Perea, and D. A. Hooftman.
577 2012. Modelling spread of British wind-dispersed plants under future wind speeds in
578 a changing climate. *Journal of Ecology* **100**:104–115.

579 Cabral, A., J. De Miguel, A. Rescia, M. Schmitz, and F. Pineda. 2003. Shrub encroach-
580 ment in Argentinean savannas. *Journal of Vegetation Science* **14**:145–152.

581 Chew, R. M., and A. E. Chew. 1970. Energy relationships of the mammals of a desert
582 shrub (*Larrea tridentata*) community. *Ecological Monographs* pages 2–21.

583 D’Odorico, P., J. D. Fuentes, W. T. Pockman, S. L. Collins, Y. He, J. S. Medeiros,
584 S. DeWekker, and M. E. Litvak. 2010. Positive feedback between microclimate and
585 shrub encroachment in the northern Chihuahuan desert. *Ecosphere* **1**:1–11.

586 D’Odorico, P., G. S. Okin, and B. T. Bestelmeyer. 2012. A synthetic review of feedbacks
587 and drivers of shrub encroachment in arid grasslands. *Ecohydrology* **5**:520–530.

588 Gandhi, S. R., E. A. Yurtsev, K. S. Korolev, and J. Gore. 2016. Range expansions
589 transition from pulled to pushed waves as growth becomes more cooperative in an
590 experimental microbial population. *Proceedings of the National Academy of Sciences*
591 **113**:6922–6927.

592 Gardner, J. L. 1951. Vegetation of the creosotebush area of the Rio Grande Valley in
593 New Mexico. *Ecological Monographs* **21**:379–403.

594 Gibbens, R., R. McNeely, K. Havstad, R. Beck, and B. Nolen. 2005. Vegetation changes
595 in the Jornada Basin from 1858 to 1998. *Journal of Arid Environments* **61**:651–668.

596 Goslee, S., K. Havstad, D. Peters, A. Rango, and W. Schlesinger. 2003. High-resolution
597 images reveal rate and pattern of shrub encroachment over six decades in New Mexico,
598 USA. *Journal of Arid Environments* **54**:755–767.

599 Grover, H. D., and H. B. Musick. 1990. Shrubland encroachment in southern New Mexico,
600 USA: an analysis of desertification processes in the American Southwest. *Climatic*
601 *change* **17**:305–330.

- 602 Hsieh, C.-I., and G. G. Katul. 1997. Dissipation methods, Taylor’s hypothesis, and
603 stability correction functions in the atmospheric surface layer. *Journal of Geophysical*
604 *Research: Atmospheres* **102**:16391–16405.
- 605 Huang, H., L. D. Anderegg, T. E. Dawson, S. Mote, and P. D’Odorico. 2020. Crit-
606 ical transition to woody plant dominance through microclimate feedbacks in North
607 American coastal ecosystems. *Ecology* **101**:e03107.
- 608 Jongejans, E., K. Shea, O. Skarpaas, D. Kelly, and S. P. Ellner. 2011. Importance of
609 individual and environmental variation for invasive species spread: a spatial integral
610 projection model. *Ecology* **92**:86–97.
- 611 Katul, G., A. Porporato, R. Nathan, M. Siqueira, M. Soons, D. Poggi, H. Horn, and
612 S. A. Levin. 2005. Mechanistic analytical models for long-distance seed dispersal by
613 wind. *The American Naturalist* **166**:368–381.
- 614 Keitt, T. H., M. A. Lewis, and R. D. Holt. 2001. Allee effects, invasion pinning, and
615 species’ borders. *The American Naturalist* **157**:203–216.
- 616 Kelleway, J. J., K. Cavanaugh, K. Rogers, I. C. Feller, E. Ens, C. Doughty, and N. Sain-
617 tilan. 2017. Review of the ecosystem service implications of mangrove encroachment
618 into salt marshes. *Global Change Biology* **23**:3967–3983.
- 619 Knapp, A. K., J. M. Briggs, S. L. Collins, S. R. Archer, M. S. BRET-HARTE, B. E.
620 Ewers, D. P. Peters, D. R. Young, G. R. Shaver, E. Pendall, et al. 2008. Shrub
621 encroachment in North American grasslands: shifts in growth form dominance rapidly
622 alters control of ecosystem carbon inputs. *Global Change Biology* **14**:615–623.
- 623 Kot, M., M. A. Lewis, and P. van den Driessche. 1996. Dispersal data and the spread of
624 invading organisms. *Ecology* **77**:2027–2042.

- 625 Lei, S. A. 1999. Ecological impacts of *Pogonomyrmex* on woody vegetation of a *Larrea*-
626 *Ambrosia* shrubland. *The Great Basin Naturalist* pages 281–284.
- 627 Lewis, M., and P. Kareiva. 1993. Allee dynamics and the spread of invading organisms.
628 *Theoretical Population Biology* **43**:141–158.
- 629 Lewis, M. A., M. G. Neubert, H. Caswell, J. S. Clark, and K. Shea, 2006. A guide
630 to calculating discrete-time invasion rates from data. Pages 169–192 *in* *Conceptual*
631 *ecology and invasion biology: reciprocal approaches to nature*. Springer.
- 632 Mabry, T. J., J. H. Hunziker, D. Difeo Jr, et al. 1978. Creosote bush: biology and
633 chemistry of *Larrea* in New World deserts. Dowden, Hutchinson & Ross, Inc.
- 634 Maddox, J. C., and S. Carlquist. 1985. Wind dispersal in Californian desert plants:
635 experimental studies and conceptual considerations. *Aliso: A Journal of Systematic*
636 *and Evolutionary Botany* **11**:77–96.
- 637 Marshall, A. K., 1995. *Larrea tridentata*. URL [https://www.fs.fed.us/database/](https://www.fs.fed.us/database/feis/plants/shrub/lartri/all.html#8)
638 [feis/plants/shrub/lartri/all.html#8](https://www.fs.fed.us/database/feis/plants/shrub/lartri/all.html#8).
- 639 Milne, B. T., D. I. Moore, J. L. Betancourt, J. A. Parks, T. W. Swetnam, R. R. Par-
640 menter, and W. T. Pockman. 2003. Multidecadal drought cycles in south-central New
641 Mexico: Patterns and consequences. Oxford University Press: New York, NY.
- 642 Moreno-de Las Heras, M., R. Díaz-Sierra, L. Turnbull, and J. Wainwright. 2015. Assess-
643 ing vegetation structure and ANPP dynamics in a grassland–shrubland Chihuahuan
644 ecotone using NDVI–rainfall relationships. *Biogeosciences* **12**:2907–2925.
- 645 Moreno-de las Heras, M., L. Turnbull, and J. Wainwright. 2016. Seed-bank structure
646 and plant-recruitment conditions regulate the dynamics of a grassland-shrubland Chi-
647 huahuan ecotone. *Ecology* **97**:2303–2318.

648 Mugasi, S., E. Sabiiti, and B. Tayebwa. 2000. The economic implications of bush
649 encroachment on livestock farming in rangelands of Uganda. *African Journal of Range*
650 *and Forage Science* **17**:64–69.

651 Nathan, R., G. G. Katul, G. Bohrer, A. Kuparinen, M. B. Soons, S. E. Thompson,
652 A. Trakhtenbrot, and H. S. Horn. 2011. Mechanistic models of seed dispersal by wind.
653 *Theoretical Ecology* **4**:113–132.

654 Neubert, M. G., and H. Caswell. 2000. Demography and dispersal: calculation and
655 sensitivity analysis of invasion speed for structured populations. *Ecology* **81**:1613–
656 1628.

657 Oba, G., E. Post, P. Syvertsen, and N. Stenseth. 2000. Bush cover and range condition
658 assessments in relation to landscape and grazing in southern Ethiopia. *Landscape*
659 *ecology* **15**:535–546.

660 Pan, S., and G. Lin. 2012. Invasion traveling wave solutions of a competitive system
661 with dispersal. *Boundary Value Problems* **2012**:120.

662 Parizek, B., C. M. Rostagno, and R. Sottini. 2002. Soil erosion as affected by shrub
663 encroachment in northeastern Patagonia. *Rangeland Ecology & Management/Journal*
664 *of Range Management Archives* **55**:43–48.

665 Peters, D. P., and J. Yao. 2012. Long-term experimental loss of foundation species:
666 consequences for dynamics at ecotones across heterogeneous landscapes. *Ecosphere*
667 **3**:1–23.

668 Ratajczak, Z., J. B. Nippert, and S. L. Collins. 2012. Woody encroachment decreases
669 diversity across North American grasslands and savannas. *Ecology* **93**:697–703.

670 Raupach, M. 1994. Simplified expressions for vegetation roughness length and zero-

- 671 plane displacement as functions of canopy height and area index. *Boundary-Layer*
672 *Meteorology* **71**:211–216.
- 673 Ravi, S., P. D’Odorico, S. L. Collins, and T. E. Huxman. 2009. Can biological invasions
674 induce desertification? *The New Phytologist* **181**:512–515.
- 675 Reed, M., L. Stringer, A. Dougill, J. Perkins, J. Athopheng, K. Mulale, and N. Favretto.
676 2015. Reorienting land degradation towards sustainable land management: Linking
677 sustainable livelihoods with ecosystem services in rangeland systems. *Journal of envi-*
678 *ronmental management* **151**:472–485.
- 679 Reynolds, J. F., R. A. Virginia, P. R. Kemp, A. G. De Soyza, and D. C. Tremmel. 1999.
680 Impact of drought on desert shrubs: effects of seasonality and degree of resource island
681 development. *Ecological Monographs* **69**:69–106.
- 682 Roques, K., T. O’connor, and A. R. Watkinson. 2001. Dynamics of shrub encroach-
683 ment in an African savanna: relative influences of fire, herbivory, rainfall and density
684 dependence. *Journal of Applied Ecology* **38**:268–280.
- 685 Schlesinger, W. H., and A. M. Pilmanis. 1998. Plant-soil interactions in deserts. *Biogeo-*
686 *chemistry* **42**:169–187.
- 687 Schlesinger, W. H., J. A. Raikes, A. E. Hartley, and A. F. Cross. 1996. On the spatial
688 pattern of soil nutrients in desert ecosystems: ecological archives E077-002. *Ecology*
689 **77**:364–374.
- 690 Schlesinger, W. H., J. F. Reynolds, G. L. Cunningham, L. F. Huenneke, W. M. Jarrell,
691 R. A. Virginia, and W. G. Whitford. 1990. Biological feedbacks in global desertification.
692 *Science* **247**:1043–1048.
- 693 Sirami, C., and A. Monadjem. 2012. Changes in bird communities in Swaziland savannas

694 between 1998 and 2008 owing to shrub encroachment. *Diversity and Distributions*
695 **18**:390–400.

696 Skarpaas, O., and K. Shea. 2007. Dispersal patterns, dispersal mechanisms, and invasion
697 wave speeds for invasive thistles. *The American Naturalist* **170**:421–430.

698 Sullivan, L. L., B. Li, T. E. Miller, M. G. Neubert, and A. K. Shaw. 2017. Density depen-
699 dence in demography and dispersal generates fluctuating invasion speeds. *Proceedings*
700 *of the National Academy of Sciences* **114**:5053–5058.

701 Taylor, C. M., and A. Hastings. 2005. Allee effects in biological invasions. *Ecology*
702 *Letters* **8**:895–908.

703 Thompson, S. E., S. Assouline, L. Chen, A. Trahktenbrot, T. Svoray, and G. G. Katul.
704 2014. Secondary dispersal driven by overland flow in drylands: Review and mechanistic
705 model development. *Movement ecology* **2**:7.

706 Trollope, W., F. Hobson, J. Danckwerts, and J. Van Niekerk. 1989. Encroachment and
707 control of undesirable plants. *Veld management in the Eastern Cape* pages 73–89.

708 Turnbull, L., J. Wainwright, and R. E. Brazier. 2010. Changes in hydrology and erosion
709 over a transition from grassland to shrubland. *Hydrological Processes: An Interna-*
710 *tional Journal* **24**:393–414.

711 Van Auken, O. 2009. Causes and consequences of woody plant encroachment into western
712 North American grasslands. *Journal of environmental management* **90**:2931–2942.

713 Van Auken, O. W. 2000. Shrub invasions of North American semiarid grasslands. *Annual*
714 *review of ecology and systematics* **31**:197–215.

715 Vasek, F. C. 1980. Creosote bush: Long-lived clones in the Mojave Desert. *American*
716 *Journal of Botany* **67**:246–255.

- 717 Veit, R. R., and M. A. Lewis. 1996. Dispersal, population growth, and the Allee ef-
718 fect: dynamics of the house finch invasion of eastern North America. *The American*
719 *Naturalist* **148**:255–274.
- 720 Wang, M.-H., M. Kot, and M. G. Neubert. 2002. Integrodifference equations, Allee
721 effects, and invasions. *Journal of mathematical biology* **44**:150–168.
- 722 Wells, P. V., and J. H. Hunziker. 1976. Origin of the creosote bush (*Larrea*) deserts of
723 southwestern North America. *Annals of the Missouri Botanical Garden* pages 843–861.
- 724 Whitford, W., E. Depree, and P. Johnson. 1980. Foraging ecology of two chihuahuan
725 desert ant species: *Novomessor cockerelli* and *Novomessor albigaster*. *Insectes Sociaux*
726 **27**:148–156.
- 727 Whitford, W. G. 1978. Structure and seasonal activity of Chihuahua desert ant commu-
728 nities. *Insectes Sociaux* **25**:79–88.
- 729 Wiernga, J. 1993. Representative roughness parameters for homogeneous terrain.
730 *Boundary-Layer Meteorology* **63**:323–363.
- 731 Wood, S. 2017. *Generalized Additive Models: An Introduction with R*. 2 edition.
732 Chapman and Hall/CRC.